ISSN 0020-4412, Instruments and Experimental Techniques, 2024, Vol. 67, Suppl. 1, pp. S33–S38. © Pleiades Publishing, Ltd., 2024.

NUCLEAR EXPERIMENTAL TECHNIQUE

Modernization of the Ion-Optical System of the VITA Accelerator[1]

G. M. Ostreinov[a,*], S. S. Savinov[a,], I. M. Shchudlo[a,***], and S. Yu. Taskaev[a,b,****]**

[a] *Budker Institute of Nuclear Physics, Siberian Branch, Russian Academy of Sciences, Novosibirsk, 630090 Russia*

[b] *Novosibirsk State University, Novosibirsk, 630090 Russia*

**e-mail: G.M.Ostreinov@inp.nsk.se*

***e-mail: S.S.Savinov@inp.nsk.su*

****e-mail: I.M.Schudlo@inp.nsk.su*

*****e-mail: S.Yu.Taskaev@inp.nsk.su*

Received November 24, 2023; revised February 27, 2024; accepted March 11, 2024

Abstract—The work considers the mode of "soft" input of an ion beam into an accelerator, in which an electrostatic Q-snout lens (preaccelerating electrode) is used. Analytical and numerical calculations of the trajectories, phase portrait, and emittance of proton and deuteron beams were carried out in the energy range 0.2–2.3 MeV. It is shown that the use of a preaccelerating electrostatic lens allows one to avoid refocusing of the beam by the strong input lens of the accelerator and improve its passage through the ion-optical path. In this focusing mode, the phase portrait of the proton beam is less sensitive to changes in current and ion energy, which is important for medical installations and for its use in other applications.

DOI: 10.1134/S0020441224701306

1. INTRODUCTION

Budker Institute of Nuclear Physics, Siberian Branch, Russian Academy of Sciences, has developed a linear electrostatic tandem accelerator of an original design, called the VITA vacuum-insulated tandem accelerator. The main application of the accelerator is to conduct comprehensive research in the field of boron neutron capture therapy (BNCT) [1]. To create a neutron beam with the intensity and energy required for BNCT, the ^{7}Li(p, n)^{7}Be reaction is used with a threshold energy of 1882 keV. The original optical system of the accelerator was designed to transport a proton beam with a current of 10 mA and an energy of more than 2 MeV. As the setup was improved, it began to be used for a number of other applications, such as surface spectroscopy using Rutherford backscattering, measurement of differential cross sections in ^{7}Li(p, α)^{4}He, ^{7}Li(p, p'γ)^{4}Li nuclear reactions, and also for radiation testing of materials using fast neutrons [1]. Thus, the accelerator must operate in the energy range of 0.2–2.3 MeV and currents in the range from 1 nA to 10 mA in various experiments. However, optimal transport of the ion beam through the accelerator is only possible in a limited range of energy values. The reason for this is the input electrostatic lens that occurs in the area where the low-energy path and the accelerator connect (Fig. 1). The focal length of such a lens f is proportional to the ratio of the energy of the injected beam to the change in intensity $f \sim 4V/\Delta E$ [2], where V is potential corresponding to the energy of ions and ΔE is change in field strength at the aperture. Due to the large gradient of the field strength between the field-free region and the accelerating gaps, where the field strength reaches 25 kV/cm, the effect on the beam optics in the accelerator is decisive. With a total accelerator length of 2 m, the focal length of the lens at a voltage of 1.15 MV on the high-voltage electrode and an injection energy of 21 keV is only approximately 5 cm and it is already approximately 54 cm at a voltage of 200 kV. Obviously, such a spread of focal lengths during accelerator operation requires an additional focusing element. In the current optical configuration, compensation for the focusing action of the input electrostatic lens is achieved by a "hard" focusing scheme (Fig. 2a), when a highly divergent ion beam of small radius is introduced into the accelerator. Such a beam can only be obtained by refocusing it using a magnetic lens immediately before entering the accelerator.

[1] Proceedings of the 28th Conference on Charged Particle Accelerators "RuPAC'23," Novosibirsk.

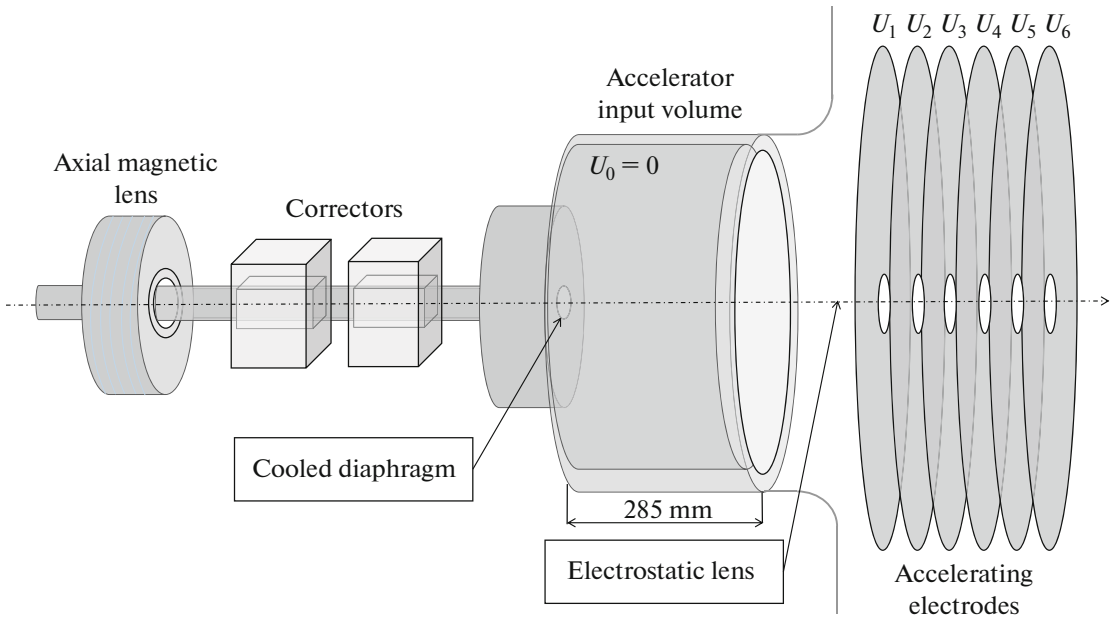

Fig. 1. Schematic diagram of the low-energy path of the VITA accelerator.

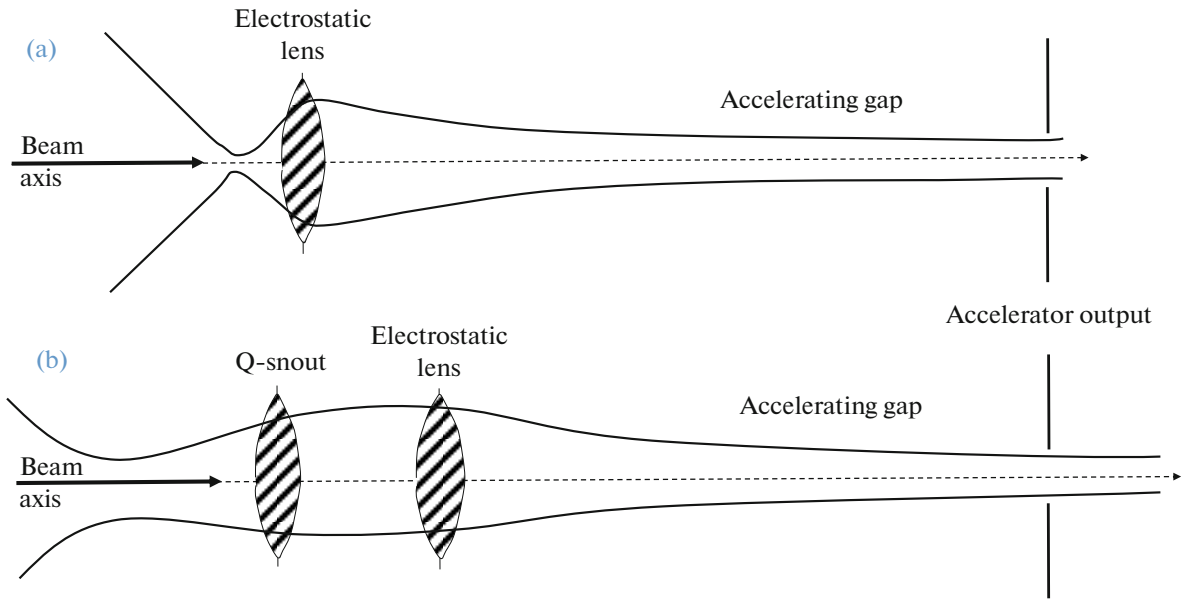

Fig. 2. Schemes of beam input into the accelerator: (a) hard focusing scheme, (b) soft input.

The article describes a modernized optical system that involves placing a so-called Q-snout lens in the input volume of the accelerator and implementing a "soft" beam input scheme (Fig. 2b). In our case, applying a voltage of 5 to 90 kV to the Q-snout lens electrode allows us to obtain a weakly converging beam with a diameter of approximately 10 mm at the accelerator output. A new optical scheme is analyzed using matrix formalism. Modeling of electric fields and beam transportation was performed, and its phase portrait and envelopes were obtained.

2. LENS DESIGN

The design diagram of the Q-snout lens is shown in Fig. 3 and consists of two coaxial cylindrical electrodes separated by a gap of 30 mm, with a total length of 175 mm. The matching electrode consists of two connected metal cylinders 30 and 95 mm long, with

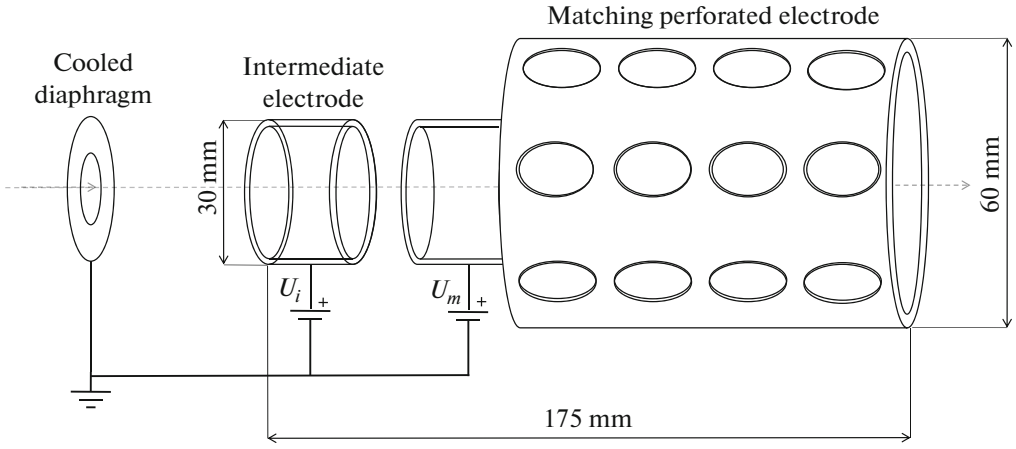

Fig. 3. Schematic diagram of the Q-snout lens.

diameters of 30 and 60 mm, respectively. The perforated structure of the matching electrode with a geometric transparency coefficient of 0.75 is due to the requirement of vacuum conductivity. A control voltage U_i and U_m is applied to the electrodes from independent power sources. The input volume is connected to the external tank of the accelerator and, together with the cooled diaphragm, is at ground potential. Note that differential pumping in the input volume of the accelerator provides a pressure in 10^{-4} Pa, which allows voltages of up to 115 kV to be applied to the lens electrodes. Using insulating ceramic rods, the lens is installed in the input volume of the accelerator along the beam axis.

Thus, when a control voltage is applied to the lens electrodes,

1. an immersion-type lens is created with focal properties determined by the ratio U_i/U_m;

2. the ion beam injected from the side of the cooled diaphragm is focused and increases its energy by an amount $e(U_m - U_i)$, which, in turn, reduces the influence of the input electrostatic lens on it;

3. the strength of the electrostatic lens is weakened by reducing the gradient of the electric field strength ΔE between the matching electrode and the first electrode of the accelerator.

3. ANALYSIS AND NUMERICAL MODELING

In this section, we formalize the problem of calculating the modernized optical system. Then, using experimental data on the beam characteristics, we will conduct a numerical simulation of beam transportation. The purpose of the calculation is to obtain the values of control voltages U_m and U_i of Q-snout lenses, which will enable beam transport through the accelerator with minimal losses and will provide a converging proton beam with a transverse size of approximately 10 mm in the energy range of 0.2–2.3 MeV at the accelerator exit. Experimental data from emittance measurements indicate that we have an ion beam with a current of 3 mA and a transverse size of 14 mm, an angular spread of ±50 mrad, and a normalized emittance $\varepsilon_{\text{norm}} = 0.20$ mm mrad at the accelerator entrance [3]. We will use this data for both numerical estimates and modeling.

Due to the small angular spread, the beam envelope can be calculated in the paraxial approximation, and the weak influence of the space charge in the acceleration region allows the optical properties of the system to be described in terms of the transition matrix for the variables $y(z)$ and $y'(z)$, where $y(z)$ (mm) is transverse size of the beam and $y'(z)$ (mrad) is the angle of inclination of the envelope to the beam axis. We will place the origin at the location of the cooled diaphragm (see Fig. 2b), then the matrix equation connecting the dimensions and angle of the beam at the entrance to the accelerator and at the exit will have the form

$$\begin{bmatrix} y(z) \\ y'(z) \end{bmatrix} = M_G M_E M_F M_S M_F \begin{bmatrix} y_0(z) \\ y_0'(z) \end{bmatrix},$$

where M_F is matrix of the free interval, M_S is Q-snout lens matrix, M_E is matrix of the input electrostatic lens, and M_G is acceleration gap matrix. To obtain the functional dependence of the beam size and angle on the control voltage, we use well-known expressions for the focal lengths of aperture and immersion lenses [4] as well as a simplified transition matrix for a multiaperture acceleration gap. In expanded form, the equation takes the form

$$\begin{bmatrix} y(z) \\ y'(z) \end{bmatrix} = \begin{bmatrix} 1 & A \\ 0 & B \end{bmatrix} \begin{bmatrix} 1 & 0 \\ -1/f_E & 1 \end{bmatrix} \begin{bmatrix} 1 & d \\ 0 & 1 \end{bmatrix} \begin{bmatrix} 1 & 0 \\ -1/f_S & 1 \end{bmatrix} \begin{bmatrix} 1 & L \\ 0 & 1 \end{bmatrix} \begin{bmatrix} y_0 \\ y_0' \end{bmatrix}.$$

Below are the expressions for the matrix components:

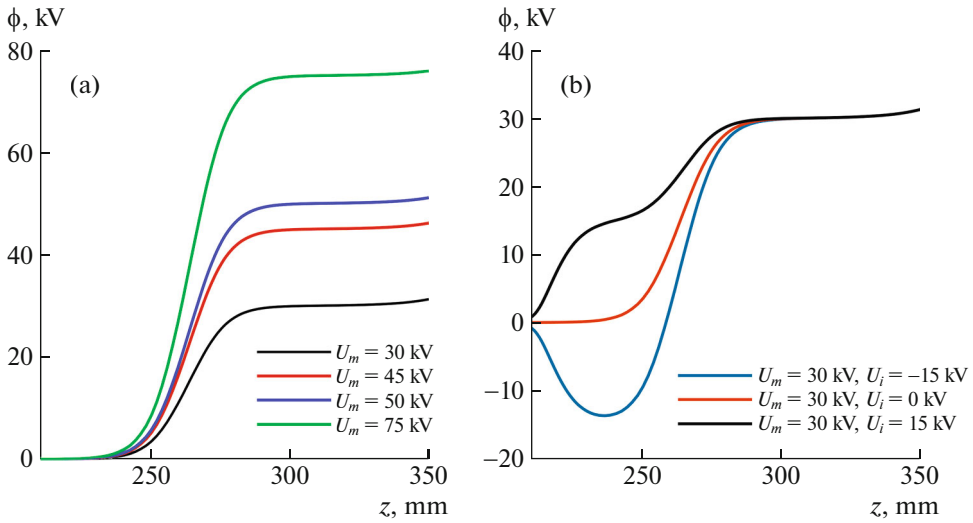

Fig. 4. Axial distribution of potential in the input volume of the accelerator for different values U_i and U_m and high voltage of 1 MV: (a) with zero potential at the intermediate electrode and (b) with voltage applied to the intermediate electrode.

$$\frac{1}{f_E} = \frac{e(E_1 - E_2)}{4(eU_m + \varepsilon_i)},$$

is focal power of the input electrostatic lens, where E_1 is field strength at the end of the matching electrode, E_2 is the field strength between the accelerator electrodes, U_i and U_m are voltages on the intermediate and matching electrodes, ε_i is beam injection energy;

$$\frac{1}{f_S} = \frac{(eU_{i+}\varepsilon_i)^2 + eU_m^2 - 2(U_m(eU_{i+}\varepsilon_i))}{4DU_m\left((eU_{i+}\varepsilon_i) + \sqrt{(eU_{i+}\varepsilon_i)eU_m}\right)},$$

is focal power of a two-electrode immersion lens, where D is gap between electrodes;

$$A = \frac{2b}{1 + \sqrt{\frac{U_6}{U_1}}}, \quad B = \sqrt{\frac{U_1}{U_6}},$$

L is the distance between the cooled diaphragm and the intermediate electrode, b is the size of the acceleration gap, and U_6 and U_1 are potentials of the first and last accelerating electrodes. Numerical analysis of the equation provides an estimate of the range of control voltage required for "soft" beam injection into the accelerator, U_m = 30–80 kV.

To obtain accurate U_m and U_i values, modeling was carried out using the finite element analysis method. The calculation consisted of two stages: first, three-dimensional distributions of electric fields were obtained, then the envelope and phase portraits of the beam were calculated. The actual size and regular dispersion of the ion beam were set in accordance with experimentally obtained data. A Gaussian distribution of particle density is chosen on the phase plane [5].

4. RESULTS AND DISCUSSION

The graphs of potential calculation are shown in Fig. 4. The matching electrode with control voltage U_m applied to it controls the power of the input lens by reducing the field strength gradient in the 400-mm region (Fig. 4b**)**. The role of the intermediate electrode is to independently control the focal length of the Q-snout lens.

Let us designate the criteria for selecting control voltages U_m and U_i for optimal beam passage:

1. throughout the entire accelerator, the transverse size of the beam does not exceed 20 mm;

2. a "soft" beam input mode is implemented, i.e., there is no need to refocus the beam at the accelerator input;

3. at the exit from the accelerator, the beam is almost parallel or weakly convergent.

Let us consider the beam envelopes when the accelerator is operating at an energy of 200 keV. It is clear from Fig. 5a that, with values U_m = 5–20 kV, we have a smoothly converging beam, which has transverse dimensions of 5–8 mm and an angular spread of ±15 mrad at the output (1800 mm), which meets the above criteria. When voltage is applied to the intermediate electrode U_i = −5 kV, the beam is additionally focused, and, with further U_i reduction, the lens goes into mode "hard" input, when the beam is refocused at the entrance to the accelerator [5].

Let us move on to considering the beam envelope at an energy of 1.15 MeV (Fig. 5c). Since the input lens power has increased, a voltage of 50–60 kV must be applied to the matching electrode, then the optical configuration of the beam will not change and we will obtain a beam with a size of 10 mm and an angular spread of ±10 mrad at the output. Finally, let us con-

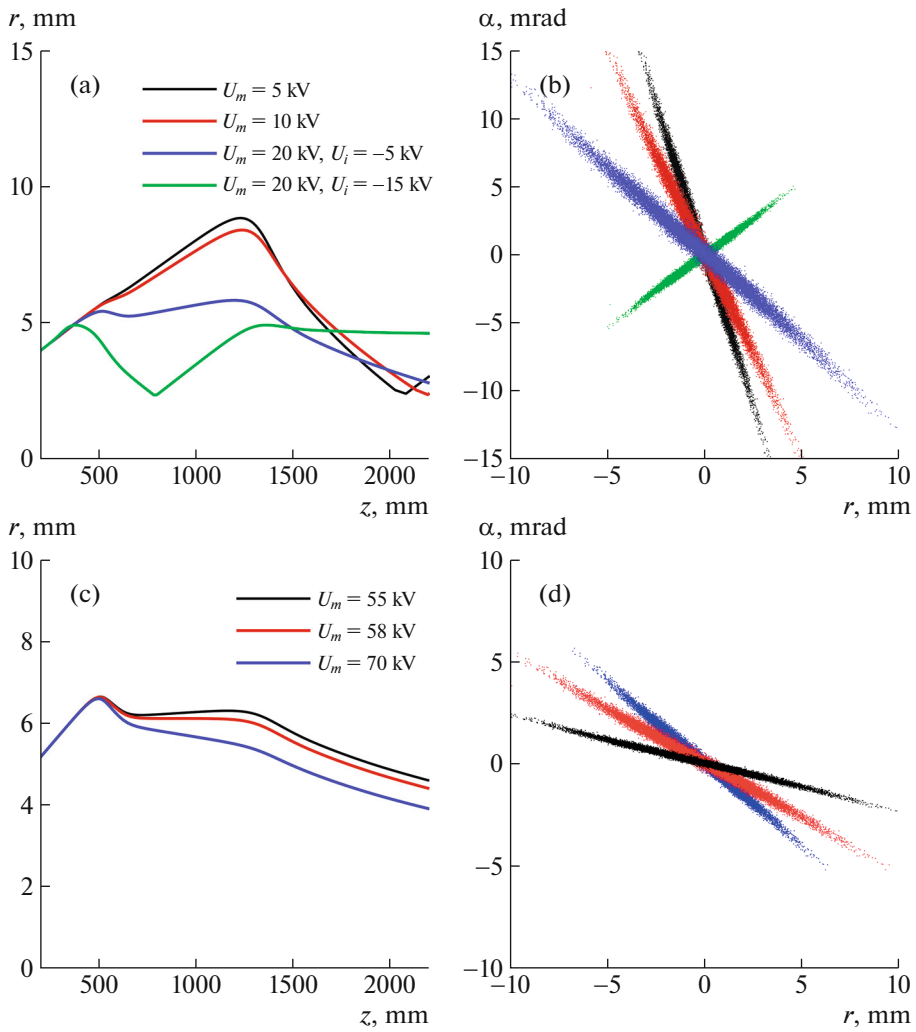

Fig. 5. Envelope and phase portraits of the proton beam at the exit from the accelerator at energies of (a, b) 200 keV and (c, d) 1 MeV.

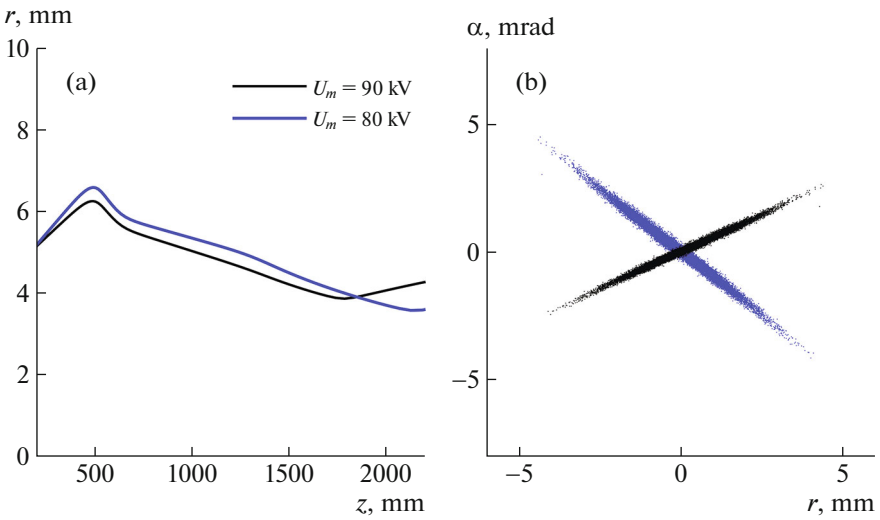

Fig. 6. (a) Envelopes and (b) phase portraits of the proton beam at the exit from the accelerator at an energy of 2.15 MeV.

sider the operation of the lens at a beam energy of 2.3 MeV, where the input lens power is greatest; as can be seen in Fig. 6a, all beams are converging, and the maximum angular spread of ±2.5 mrad is obtained when applying a voltage of 90 kV to the matching electrode.

5. CONCLUSIONS

To use the VITA tandem electrostatic accelerator in various applications, it is necessary to ensure that the beam passes through the accelerator in the energy range of 0.2–2.3 MeV. A characteristic feature of many electrostatic accelerators is a strong entrance lens that naturally occurs at the junction of the field-free region and the accelerating gap. In the current configuration of the setup, a "hard" focusing scheme is used to compensate for the effect of the input lens, where a solenoidal magnetic lens refocuses the ion beam into the region of the input lens. Since the input lens power depends on the magnitude of the high-voltage voltage, this scheme has a number of disadvantages [3]:

1. the need for precise adjustment of the focal length when the accelerator operates at different energies;

2. large spherical aberrations of the beam;

3. increased thermal load on the diaphragm of the first accelerating electrode.

In this work, it is proposed to implement a "soft" beam input scheme by installing a two-electrode Q-snout lens into the input volume of the accelerator. In a "soft" focusing scheme, the effect of the input lens is weakened by a smooth increase in the electric field at the accelerator input, and the intensity gradient is controlled by the voltage on the matching electrode U_i. In this case, the angle of inclination of the beam envelope at the entrance to the accelerator is close to zero. The advantages of this scheme compared to "hard" focusing are the lower sensitivity of the transmission coefficient and output parameters of the beam to the convergence angle of the beam at the entrance to the accelerator. Analysis of the equations and calculation of the optical path using the finite element method made it possible to determine the range of voltage values on the matching and intermediate electrodes required to implement "soft" beam input in the energy range of 0.2–2.15 MeV. The range of voltage values was (10–90) kV for U_m and (–15–5) kV for U_i. In all cases, it was possible to form a weakly converging or parallel beam at the exit from the accelerator. The maximum angular spread of ±5 mrad and transverse size of 5 mm were obtained at an accelerator energy of 2.3 MeV. In other cases, the average beam size at the accelerator exit was 4 mm and the angular spread was ±2.5 mrad.

FUNDING

The study was supported by the Russian Science Foundation (grant no. 19-72-30005, https://rscf.ru/project/19-72-30005/).

CONFLICT OF INTEREST

The authors of this work declare that they have no conflicts of interest.

REFERENCES

1. Kasatov, D.A., Koshkarev, A.M., Makarov, A.N., Ostreinov, G.M., Taskaev, S.Yu., and Shchudlo, I.M., *Instrum. Exp. Tech.,* 2020, vol. 63, no. 5, pp. 611–616. https://doi.org/10.1134/S0020441220050152
2. Elkind, M.M., *Rev. Sci. Instrum.,* 1953, vol. 24, no. 2, p. 129. https://doi.org/10.1063/1.1770640
3. Bikchurina, M.I., Bykov, T.A., Kolesnikov, Ya.A., Makarov, A.N., Ostreinov, G.M., Savinov, S.S., Taskaev, S.Yu., and Shchudlo, I.M., *Instrum. Exp. Tech.,* 2022, vol. 65, no. 4, pp. 551–562. https://doi.org/10.1134/S0020441222040169
4. Liebl, H., *Applied Charged Particle Optics,* Berlin, Heidelberg: Springer, 2007, p. 131. https://doi.org/10.1007/978-3-540-71925-0
5. Bykov, T.A., Kasatov, D.A., Kolesnikov, Ya.A., Koshkarev, A.M., Makarov, A.N., Ostreinov, Yu.M., Sokolova, E.O., Taskaev, S.Yu., and Shchudlo, I.M., *Tech. Phys.,* 2021, vol. 66, no. 1, pp. 98–103. https://doi.org/10.1134/S1063784221010047
6. Larson, J.D., *Nucl. Instrum. Methods,* 1974, vol. 122, p. 53. https://doi.org/10.1016/0029-554X(74)90471-6